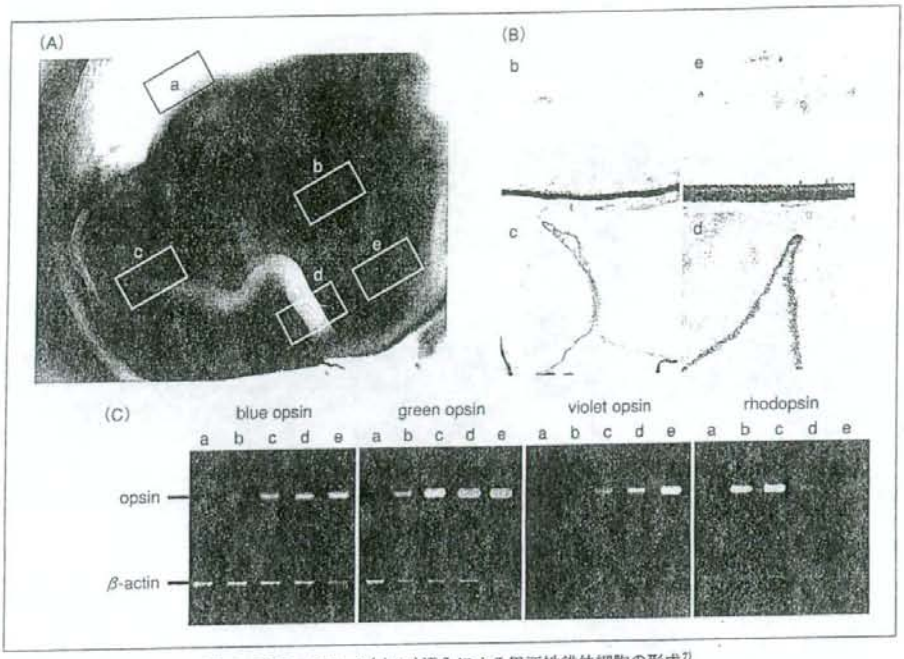

図 8 鶏胚へのPax6(+5a)導入による異所性錐体細胞の形成[7]

2 日胚に導入，19 日胚の所見．A：網膜が過剰に発育した襞を形成．この襞内では，周辺部(c)に本来は少ないオプシンをもつ錐体細胞が形成されている．B：免疫染色，C：RT-PCR．

進しており，Pax6 は網膜の成長を担っていると考えられた[7]．

つぎに，エクソン 5a を含む Pax6(+5a)を導入すると網膜から硝子体腔へ茎状構造が立ちあがった．これはすべて網膜であり，神経細胞と神経線維で構成されていた．茎状に伸びた組織では網膜が管状になっており，しかも視細胞から神経節細胞に至る層構造がほぼ形成されていた(図 7-B)．また，網膜が硝子体腔へ折りたたまれる所見もみられた(図 7-C)．網膜が水平方向へ過剰に発育し，抵抗の少ない硝子体腔へ伸展したと考えられる．

したがって，網膜を成長させる働きは Pax6(−5a)より Pax6(+5a)のほうがはるかに強いことが明らかになった．さらに，錐体視細胞が少なく杆体細胞がおもに存在する網膜周辺部に Pax6(+5a)を導入すると，異所性に錐体細胞の形成が観察された(図 8)[7]．この Pax6(+5a)による網膜の発育と錐体細胞の分化が硝子体腔へ突出せず網膜内の 1 カ所に集中すれば，黄斑になるのかもしれない．

Pax6 を入れた領域の眼球は拡大し，角膜と水晶体が対側へ偏位した．この作用は Pax6(−5a)より Pax6(+5a)のほうが強かった(図 6-A，図 7-A)[7]．眼球は発生初期には頭の横にあり，鼻側と耳側が同じ大きさであるが，発生が進むと眼球の位置が頭の横から顔の前へ向くとともに耳側が大きくなる．網膜の成長が進むと眼球が成長し，一方，網膜の形成不全では小眼球になることから，眼球の大きさには網膜の成長が関わっている．眼球の耳側が鼻側に比べて大きいのは Pax6(+5a)が耳側後極で強く発現して網膜の発育を進めるためであると考えられる．Pax6 にこのエクソン 5a が現れたのは脊椎動物になってからであるが，魚類で網膜の構造は急速に複雑化し，黄斑が生まれたのは，このエクソン 5a の追加が関与したことも示唆される．

Pax6などの眼形成遺伝子を用いた網膜の再生

Pax6/eyeless を異所導入すると昆虫ではほぼ完

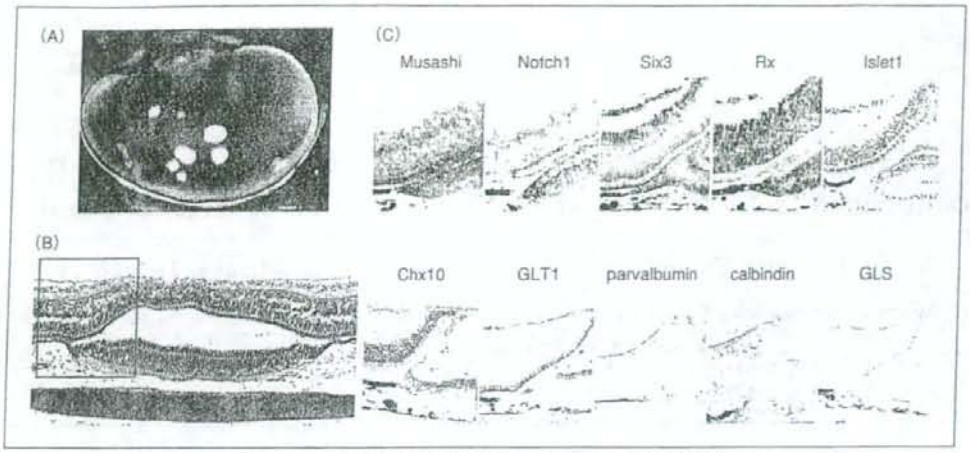

図 9　Pax6の導入による網膜色素上皮から網膜への分化転換[17]

3 日胚に導入，14 日胚の所見．遺伝子が導入された色素上皮は斑状に(A)，網膜へ分化転換している(B)．この異所網膜は *in situ* hybridization や免疫染色で網膜固有の遺伝子・蛋白発現がみられ(C)，ほぼ完全な層構造をもつが，層の方向は眼杯が折りたたまる向きに応じて本来の網膜と背合わせになっている．

全な複眼が形成される[2]．Pax6/eyeless 下流の eyes absent, sine oculis/Six, dachshund, Rx, teashirt の導入では小さい複眼が形成されるが[9-12]，哺乳類では，Pax を導入してもアフリカツメガエルの幼生で不完全な構造の異所眼が形成されるにすぎない[13]．また，Six6，Rx を発生期の脳や網膜色素上皮に導入すると，不完全ながら網膜組織が形成されるが[14-16]，Pax6 を導入するとかなり完全な層構造をもつ網膜を形成することができる(図 9)[17]．この網膜形成における Pax6(−5a)と Pax6(+5a)の働きの違いは現在検討中であるが，過去の研究からみて Pax6(+5a)のほうがより高度な網膜を形成できる可能性がある[7]．

近年，網膜色素変性症モデル動物や患者で，障害された黄斑部網膜下に胎児網膜を移植して視力が改善したことが報告された[18,19]．未熟な胎児網膜がレシピエント網膜内で分化し，シナプスを形成すると思われる．網膜色素変性症では視細胞以外の網膜構造はある程度温存されており，胎児網膜由来の視細胞のシナプスがつながったと推測される．自己の虹彩や色素上皮に網膜の形態形成遺伝子を導入あるいは発現誘導して網膜を再生できれば，やや不完全な構造であっても，このような網膜移植に利用できることが期待される．

おわりに

網膜の重症疾患で悩まされている患者や医師にとって，網膜を再生させて失われた視覚を復元させる医療は大きな夢である．しかし，構造が複雑な網膜をシナプスごと再構築することが難しく，中枢への神経投射を的確に復元しないかぎり有用な視力が得られない．できても，せいぜい光覚や手動弁の視力あるいは視野をすこし広げる程度と考えられていた．しかし，近年の再生医学研究によって視覚の復元への道はすこしずつ着実に進歩している．黄斑を形成する遺伝子システムを解明して再生医療に利用すれば，高度な視覚構造が復元できると期待される．

文献

1) Ton, C. T. T. et al. : *Cell*, **57** : 1059-1074, 1991.
2) Callaerts, P. et al. : *Annual. Rev. Neurosci.*, **20** : 483-532, 1997.
3) Nishina, S. et al. : *Br. J. Ophthalmol.*, **83** : 723-727, 1999.
4) Azuma, N. et al. : *Nat. Genet.*, **13** : 141-142, 1996.
5) Azuma, N. et al. : *Am. J. Hum. Genet.*, **65** : 656-663, 1999.
6) Azuma, N. et al. : *Am. J. Hum. Genet.*, **72** : 1565-1570, 2003.
7) Azuma, N. et al. : *Hum. Mol. Genet.*, **14** : 735-745, 2005.
8) Schedl, A. et al. : *Cell*, **86** : 71-82, 1996.

Available online at www.sciencedirect.com
ScienceDirect
Vision Research 48 (2008) 273–280
Vision Research
www.elsevier.com/locate/visres

Comparison of focal macular cone ERGs in complete-type congenital stationary night blindness and APB-treated monkeys ☆

Mineo Kondo *, Shinji Ueno, Chang-Hua Piao, Yozo Miyake, Hiroko Terasaki

Department of Ophthalmology, Nagoya University Graduate School of Medicine, 65 Tsuruma-cho, Showa-ku, Nagoya 466-8550, Japan

Received 1 August 2007; received in revised form 9 November 2007

Abstract

Focal macular cone electroretinograms (ERGs) and multifocal ERGs were recorded to study the macular function in patients with the complete-type of congenital stationary night blindness (cCSNB). The waveforms of the focal macular cone ERGs and the on- and off-responses of the multifocal ERGs in the cCSNB patients were similar to those recorded from monkey retinas treated with L-2 amino-4-phosphonobutyric acid (APB), suggesting that patients with cCSNB have a complete defect of the on-pathway even in the central retina. The results also demonstrated that there was a paradoxical positive response in the central retina of cCSNB patients, as compared to the negative full-field ERGs in the same subjects.

Keywords: Electroretinogram (ERG); Focal macular cone ERG; Congenital stationary night blindness (CSNB); Complete-type; APB (L-2 amino-4-phosphonobutyric acid)

1. Introduction

The complete-type of congenital stationary night blindness (cCSNB) is a non-progressive retinal disease characterized by congenital night blindness with a moderate decrease of the visual acuity and myopia (Miyake, Horiguchi, Suzuki, Kondo, & Tanikawa, 1997; Miyake, Yagasaki, Horiguchi, Kawase, & Kanda, 1986). The inheritance pattern of cCSNB is usually X-linked or autosomal recessive. It was recently reported that most X-linked cCSNB resulted from mutations in the *NYX* gene (Bech-Hansen et al., 2000; Pusch et al., 2000), and some cases of autosomal recessive cCSNB resulted from mutations in the *MGR6* gene (Dryja et al., 2005).

cCSNB patients have very characteristic electroretinograms (ERGs). When elicited by a bright stimulus after dark-adaptation, the ERGs are the negative-type with an a-wave of normal amplitude and a b-wave that is smaller than the a-wave. When a long-duration photopic stimulus is used, the b-waves of the ERGs of cCSNB patients are severely reduced while the off-response d-wave is well-preserved (Houchin, Purple, & Wirtschafter, 1991; Miyake, Yagasaki, Horiguchi, & Kawase, 1987; Young, 1991). These ERG waveforms are very similar to those in the monkey photopic ERGs after an intravitreal injection of 2-amino-4-phosphonobutyric acid (APB), which blocks neurotransmission from photoreceptors to the on-bipolar cells (Evers & Gouras, 1986; Knapp & Schiller, 1984; Sieving, Murayama, & Naarendorp, 1994). These results demonstrated that the defect in the neural pathway of cCSNB patients lies in the signal transmission from the photoreceptors to the depolarizing on-bipolar cells (DBCs) in both the rod and cone pathways. Recent ERG analysis using sinusoidal and ramping on/off flicker stimuli also indicated that the deficit in eyes with cCSNB is localized to the DBC pathway with no apparent involvement of the hyperpolarizing off-bipolar cells (HBCs) (Khan et al., 2005).

☆ *Grant support:* Grant-in Aid 14770952 (M.K.), and 14370557 (H.T.) from the Ministry of Education, Science, Sports and Culture, Japan.
* Corresponding author. Fax: +81 52 744 2278.
E-mail address: kondomi@med.nagoya-u.ac.jp (M. Kondo).

0042-6989/$ - see front matter © 2007 Elsevier Ltd. All rights reserved.
doi:10.1016/j.visres.2007.11.010

Although there are many electrophysiological studies on the full-field ERG in patients with cCSNB, there are very few studies on the macular function of eyes with cCSNB using either the multifocal or focal macular cone ERG techniques (Kondo et al., 2001; Leifert, Todorova, Prunte, & Palmowski-Wolfe, 2005). During our extensive studies of the complete and incomplete type of CSNB, we have been gaining the impression that the cone on-pathway may be functioning relatively well only in the central retina in cCSNB because these patients have relatively good visual function in the central field (Miyake et al., 1997; Terasaki et al., 1999).

The purpose of this study was to investigate the macular function of patients with cCSNB in more detail using focal macular cone ERGs and multifocal ERGs. To accomplish this, we separated the on- and off-responses of the photopic ERGs using long-duration photopic stimuli in the macular area of patients with cCSNB, and then compared the obtained waveforms with those recorded from monkey retinas in which the on-pathway was completely blocked pharmacologically by an intravitreal injection of L-2 amino-4-phosphonobutyric acid (APB).

2. Materials and methods

2.1. Patients with complete-type CSNB

From the patients with cCSNB examined in our clinic (Department of Ophthalmology, Nagoya University Hospital), we selected three patients who agreed to participate and were cooperative with the electrophysiological examinations (Table 1). All patients had poor night vision from birth and had no fundus abnormalities except for myopic changes. Their corrected visual acuities were 0.4, 0.4, and 0.6, and the rod branch of the dark-adaptation curve was missing as determined by psychophysical dark adaptometry. The full-field ERG rod responses were undetectable, and the rod and cone mixed maximal ERG had a negative-shape with no detectable oscillatory potentials.

An informed consent was obtained from the three patients after a full explanation of the procedures. All studies were conducted in accordance with the principles embodied in the Declaration of Helsinki.

2.2. Animals

Four rhesus (*Macaca mulata*) monkeys were studied under protocols approved by Nagoya University School of Medicine. All experiments were conducted in accordance with NIH guidelines on animal use and with the ARVO statement on the Use of Animals in Ophthalmic and Vision Research. The animals were anesthetized with intramuscular injection of ketamine hydrochloride (7 mg/kg, 5–10 mg/kg/h maintenance dose) and xylazine (0.6 mg/kg). The respiration and heart rate were monitored, and hydration was maintained by a slow, continuous infusion of lactated Ringer solution. The cornea was anesthetized by topical 1% tetracaine, and the pupil was dilated with topical 0.5% tropicamide, 0.5% phenylephrine HCL, and 1% atropine.

2.3. Drug application to animals

The drugs were injected into the vitreous with a 30-gauge needle inserted through the pars plana approximately 3 mm posterior to the limbus. The drugs (Sigma Chemical Co., St. Louis, MO) were dissolved in sterile saline and injected in amounts of 0.05–0.07 ml. The intravitreal concentration was 1–2 mM for L-2 amino-4-phosphonobutyric acid (APB) and 5 mM for *cis*-2, 3 piperidine dicarboxylic acid (PDA). Recordings were begun about 60–90 min after the drug injections, and studies were completed within 5 h. Although the drug effects are mostly reversible after a recovery period of several weeks, the results that are presented were recorded from the eyes not previously treated.

2.4. Focal macular cone ERG

Focal macular cone ERGs were elicited by stimulating the macula with small stimulus spots (Miyake, 1988b; Miyake, Shiroyama, Ota, & Horiguchi, 1988a). The position of the spot on the fundus was monitored during the recording with a modified infrared fundus camera. The Burian-Allen bipolar contact lens electrode (Hansen Ophthalmic Development Laboratories, Iowa City, IA) which was used to record the focal macular cone ERGs, allowed a clear view of the fundus on the television monitor. The luminances of the stimulus and the background were 30.0 cd/m^2 and 3.0 cd/m^2, respectively. A 5-Hz rectangular stimulus (100 ms-on and 100 ms-off) was used with a stimulus spot of 15 degrees in diameter. A total of 512 responses were averaged by a signal processor, and the time constant was 0.03 s with a 300-Hz high-cut filter. The ERG responses produced by this method are generated by the cone system, and the responses elicited by the spot stimuli are considered to be local responses (Miyake, 1988b; Miyake et al., 1988a).

2.5. Recording multifocal on- and off-responses

Our method for recording on- and off-responses of the multifocal ERGs has been described in detail (Kondo & Miyake, 2000; Kondo, Miyake, Horiguchi, Suzuki, & Tanikawa, 1998). In brief, multifocal ERGs were obtained with the VERIS system (EDI, San Mateo, CA). The stimulus array consisted of 61 hexagonal elements that were displayed on a CRT monitor (GDM, Sony, Tokyo, Japan) and driven at 75 frames/s. At a viewing distance of 27 cm, the subtense of the visual field was approximately 50°.

To obtain on- and off-responses with the VERIS system, we used consecutive white TV frames. Each hexagon was modulated between two stimulus patterns according to a binary m-sequence: eight consecutive white frames followed by eight consecutive dark frames (pattern A) or 16 consecutive dark frames (pattern B). In this stimulus setting, a stimulus is not continuously bright during its bright phase because the focal flash decays within a few milliseconds. However, there is evidence that a high-frequency train of flashes can roughly simulate the effects produced by a long-duration stimulus and thus can produce a corneal positive off-response (Saeki & Gouras, 1996; Young, 1991).

Based on our preliminary study, the following stimulus parameters were found to be suitable for eliciting maximal on- and off-responses from each local retinal area: stimulus intensity of 120 cd/m^2 with a duration of 8 frames (106 ms) on a 20 cd/m^2 background illumination. The m-sequence stimulation rate was, therefore, 4.7/s and the base interval was 213.3 ms (Kondo & Miyake, 2000; Kondo et al., 1998).

Table 1
Clinical characteristics of three patients with complete type CSNB

Case	Age	Sex	Inheritance pattern	Refractive error (*D*)	Visual acuity
Case 1	54	M	Autosomal recessive	−4.0	0.4
Case 2	20	M	X-linked	−9.5	0.4
Case 3	15	F	Autosomal recessive	−6.0	0.6

The signals were amplified by 100 K and filtered between 3 and 300 Hz (Grass, Quincy, MA). The data sampling rate was 1200 Hz. To reduce the artifacts due to eye movements, an "artifact rejection" algorithm (VERIS software, EDI) was used once (Marmor et al., 2003). The length of the m-sequence used was 2^{11}–1. Thus, the total recording took 7.3 min, and it was divided into 16 segments.

For recording multifocal ERGs from monkeys, a modified ophthalmoloscopic technique was used to locate the projection of the fovea on the center of the stimulus pattern (Rangaswamy, Hood, & Frishman, 2003). This modified ophthalmoscope was kindly provided by Dr. L. Frishman (University of Houston). The position of the fovea was checked frequently before and after the multifocal ERG recordings.

2.6. Recording full-field ERGs

Full-field ERGs were recorded with long-duration stimuli (166 ms or 100 ms) using a densely-packed array of 102 green LEDs (525 nm peak wavelength; 50 nm at half-amplitude). The array was positioned at the top of the Ganzfeld dome and covered by a diffuser (Ueno et al., 2006). The LEDs were controlled by a digital function generator (WF1945, NF Corporation, Tokyo, Japan). The stimulus intensity and background illumination measured in the dome was 120 cd/m^2 and 40 cd/m^2, respectively. In the last experiment, the stimulus intensity and background illumination was set at 30 cd/m^2 and 3 cd/m^2, respectively, in order to compare the waveforms of full-field ERG and focal macular cone ERG at the same stimulus and background condition.

After 10 min of light adaptation, ERGs were recorded with a Burian-Allen bipolar contact lens electrode (Hansen Ophthalmic Development Labs, Iowa City, IA). A ground electrode was attached to the ipsilateral ear. Responses were amplified by 10 K and the bandpass was set to 0.3–1000 Hz. The data were digitized at 4.3 kHz. Twenty responses were averaged (Power Lab, AD Instruments, Castle Hill, Australia).

3. Results

3.1. Focal macular cone ERGs in cCSNB

Representative focal macular cone ERGs recorded from a myopic control (38-year-old man; refractive error, −5.50 D) and the three patients with cCSNB are shown in the left panel of Fig. 1. The waveforms from the three patients are clearly different from those of the myopic control: the amplitudes of the a-waves are normal, but the amplitudes of the following positive wave are smaller than the b-wave of the myopic control (see also Table 2). These changes resulted in a reduced b-wave to a-wave (b/a) ratio. In addition, the implicit times of the a- and b-waves in

Table 2
Amplitudes and implicit times of focal macular ERGs (FMERGs) from three patients with complete type CSNB and 15 patients with myopic controls

	Amplitude (μV)			Implicit times (ms)	
	a-wave	b-wave	b/a ratio	a-wave	b-wave
Case 1	2.4	2.4	1.0	21.4	47.2
Case 2	1.9	2.9	1.56	28.0	46.8
Case 3	2.4	3.1	1.29	28.0	59.5
Myopic controls ($n = 15$)	2.0 ± 0.5	5.1 ± 0.9	2.51 ± 0.44	19.6 ± 1.7	40.9 ± 3.0

Data in myopic controls are expressed as the mean ± SD.

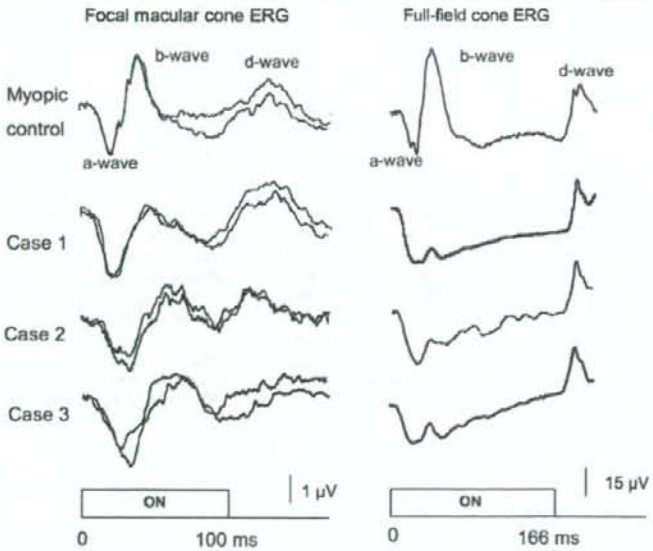

Fig. 1. Focal macular cone ERGs (left panel) and full-field ERGs (right panel) elicited by long duration stimuli recorded from a myopic control and three patients with complete-type congenital stational night blindness (cCSNB). Note that the amplitude ratios of the positive wave to the a-wave was <1.0 for the full-field ERG, but >1.0 for focal macular cone ERGs in the cCSNB patients.

cCSNB patients were prolonged (Table 2). The d-waves seen at the offset of the stimulus was not so prominent for both myopic controls and patients.

The full-field, photopic ERGs elicited by a long-duration stimulus (166 ms) from the same subjects are shown in the right panel of Fig. 1. In all three cCSNB patients, the b/a amplitude ratio was clearly <1.0 resulting in a "negative" ERG waveform.

3.2. Focal macular cone ERGs in monkey retina after APB

It is known that the on-response b-wave of the photopic long-flash ERG originates mainly from the neural activity of the cone depolarizing bipolar cells (DBCs) (Knapp & Schiller, 1984; Sieving et al., 1994). Based on the focal macular cone ERGs in the cCSNB patients, we thought that the function of cone on-pathway may be preserved to some degrees in the central retina of the cCSNB patients. To test this hypothesis, it was necessary to record the focal macular cone ERGs from the monkey retina after the cone on-pathway was completely blocked pharmacologically by APB, and to compare these waveforms with those from cCSNB patients.

The focal macular cone ERGs recorded from two rhesus monkeys before and after intravitreous injection of APB are shown in Fig. 2. After the APB injection, the a-wave amplitude became larger, and the peak time of the a- and the following positive wave became prolonged. The d-wave was slightly enhanced after APB. The ratio of the b-wave to the a-wave amplitudes became smaller than controls, but was still larger than 1.0 (monkey #1, 1.24; monkey #2, 1.33).

We initially interpreted this to indicate that remaining positive wave might be caused by an incomplete blockage of APB and thus injected more APB. However, the addition of APB did not change the waveforms of the focal macular cone ERGs, and the b/a amplitude ratio still remained greater than 1.0 even after increasing the APB concentration to twice the original concentration (2 mM).

The similarity in the waveforms between cCSNB patients and monkeys treated with APB indicated that the cone on-pathway seemed be completely blocked even in the central retina in cCSNB.

3.3. Multifocal on- and off-responses in cCSNB and APB-treated monkey

We also noted that the waveforms of photopic ERG with long duration stimuli were different between full-field cone ERGs and focal macular cone ERGs in cCSNB patients; the amplitude of remaining positive wave was still larger than that of the a-wave, whereas the amplitude ratio of the positive wave to the a-wave was always less than 1.0 for the full-field ERGs (Fig. 1). However, these differences in the waveform could be due to the different stimulus and recording conditions in the two methods. Therefore, we next compared these waveforms between the central and peripheral retinas directly in a patient with cCSNB. For

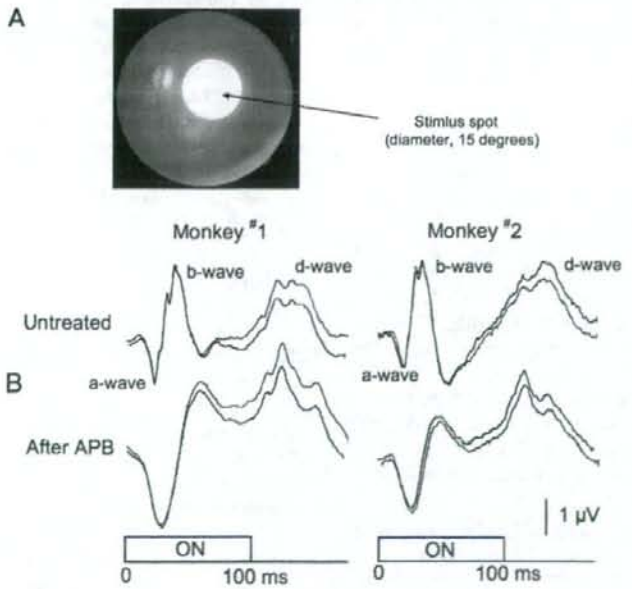

Fig. 2. Stimulus location and focal macular cone ERGs recorded from two monkeys. (A) Fundus photographs showing the stimulus spot. The 15° stimulus spot (diameter) was focused on the fovea. (B) Waveforms of focal macular cone ERGs before and after intravitreal injection of APB for two rhesus monkeys. Intravitreous concentration of APB was 1.0 mM.

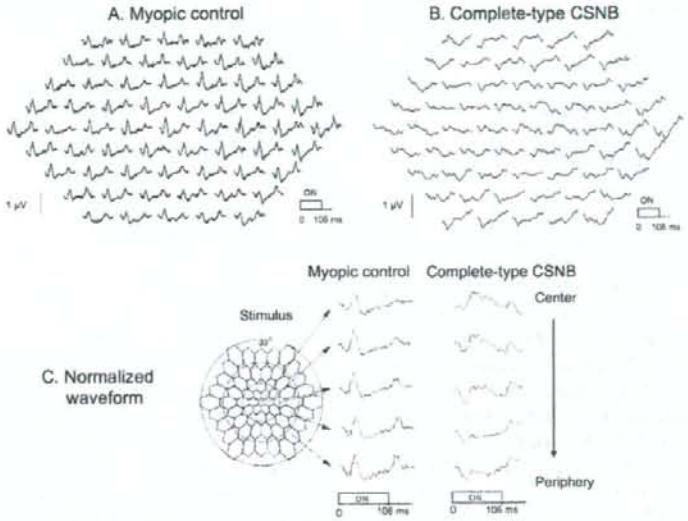

Fig. 3. Multifocal on- and off- responses using eight consequtive white frames. (A) Results from a myopic control. (B) Results from a patient with cCSNB (Case 1). (C) Normalized waveforms from five eccentric rings. Note that in cCSNB, the amplitude ratio of the positive wave to the a-wave is >1.0 in the central retina, but gradually become smaller towards to the periphery.

this purpose, we recorded the multifocal on- and off-responses (Kondo & Miyake, 2000; Kondo et al., 1998).

The multifocal on- and off-responses recorded from a representative myopic control (A), and a patient with cCSNB (B, Case 1 of Table 1) are shown in Fig. 3. It was clear that when compared to myopic control, the amplitudes of the positive wave are reduced at all locations in cCSNB. However, the amplitude of the positive wave is relatively preserved in the central retina, and the relative amplitude of the positive wave to the a-wave became small from the center to the periphery. The changes in the waveforms were clearly seen when the responses were grouped for each eccentric rings (Fig. 3C). The remaining positive wave is well preserved in the central retina, but gradually became smaller towards the peripheral retina. The amplitude ratio of the positive wave to the a-wave was >1.0 in the central retina, but <1.0 in the periphery. These findings are consistent with our combined findings of full-field ERG and focal macular cone ERGs in patients with cCSNB.

We also confirmed these results in a monkey retina after treatment with APB (Fig. 4). The remaining positive response was relatively large in the central retina, but the relative ratio of the positive wave to the a-wave gradually became smaller towards the periphery (Fig. 4C). These findings were quite similar to those in patients with cCSNB.

3.4. Origin of the remaining positive wave of photopic ERG at central retina

One question that still remained was the origin of the remaining positive component of the focal macular cone ERG seen even after blockage of cone on-pathway. To study the retinal origin of this component, we added PDA to block the neural activities of post-synaptic off-pathways and horizontal cells in monkeys. Fig. 5 shows the changes in the waveforms of photopic ERG with long duration stimulus before and after APB and PDA application for full-field and focal macular cone ERGs in a rhesus monkey. In this experiment, the same stimulus (30 cd/m^2) and background (3 cd/m^2) intensities were used for both full-field and focal macular cone ERGs, because the waveform of photopic ERG is dependent on the stimulus and background intensities (Kondo et al., 2000; Ueno, Kondo, Niwa, Terasaki, & Miyake, 2004). We found that after the PDA injection, the remaining positive wave of focal macular cone ERGs completely disappeared (lower traces of Fig. 5).

4. Discussion

We compared the waveform of focal macular cone ERGs recorded from cCSNB patients with those from APB-treated monkeys, and found that the waveforms were very similar: the amplitude of the a-wave was normal or slightly larger than control; a positive wave was still present after the a-wave, and the amplitude of this positive wave was larger than that of the a-wave; and the implicit time of the positive wave was delayed. These similarities in the waveform of focal macular ERG between the cCSNB patients and APB-treated monkeys suggested that the cone on-pathway is nearly completely blocked even in the central retina of the cCSNB patients.

Although the waveform of the a-wave and the following positive wave were very similar for cCSNB patients and

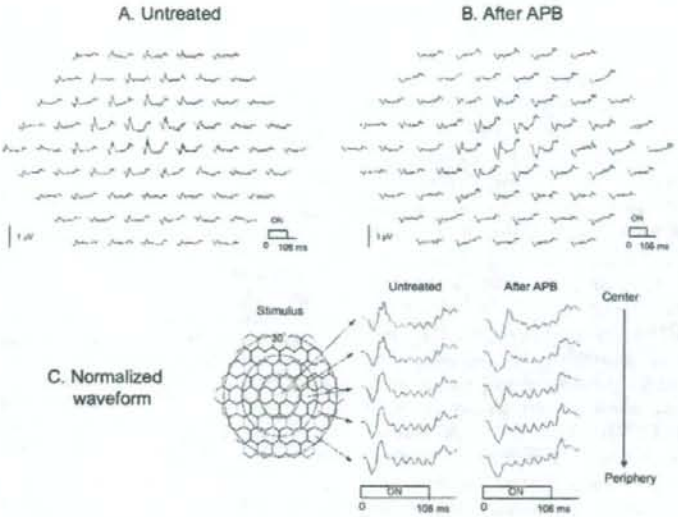

Fig. 4. Multifocal on- and off-responses before and after intravitreous injection of APB in a rhesus monkey. Intravitreous concentration of APB was 1.0 mM. Unstretched hexagonal elements (same size) are used for these monkey experiments. (A) Multifocal ERGs before APB. (B) Multifocal ERG after APB. (C) Normalized waveforms from five eccentric rings after APB application. The waveform after APB are very similar to those recorded from cCSNB patients.

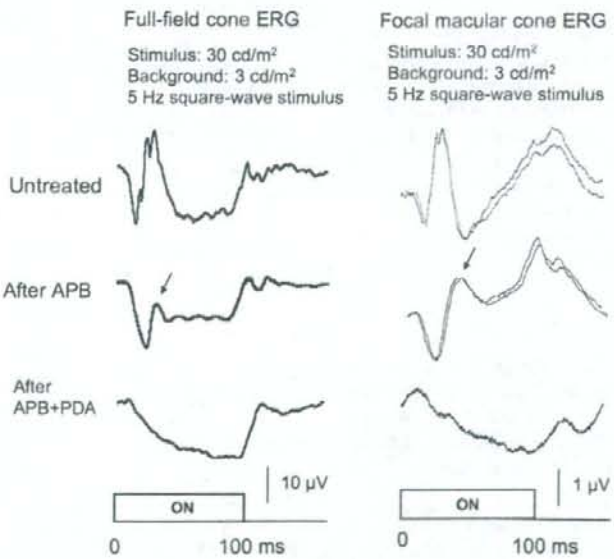

Fig. 5. Comparison in the waveforms of photopic ERG with long duration stimulus before and after APB and PDA application for full-field and focal macular cone ERGs in a rhesus monkey. Five hertz square-wave flickering stimulus of 30 cd/m^2 was presented on a background illumination of 3 cd/m^2 for both ERGs. After APB and PDA, the remaining positive wave at stimulus onset disappears completely for both ERGs (arrows).

APB-treated monkeys, the waveform of the d-wave at the offset of the stimulus was slightly different: the amplitude of the d-wave of the focal macular cone ERG was enhanced after the intravitreal injection of APB in monkeys, whereas the d-wave of focal macular cone ERG in cCSNB patients was not larger than that of myopic control. We do not know the reason for this difference in the waveform of the d-wave between the cCSNB patients and

APB-treated monkeys. However, it may be partly due to the differences between inherited human disease and the pharmacological animal model.

Although our electrophysiological study showed functional similarity between the retina of patients with cCSNB and APB-treated monkey retinas, there still remained the question of whether the retinal on-pathway is completely blocked in the retina of patients with cCSNB. Two psychophysical studies suggested that rod on-pathway may not be completely blocked in cCSNB patient (Allen et al., 2003; Young, Price, & Harrison, 1986).

We also found that even after a complete blockage of the cone on-pathway, there still remained a sizeable positive wave of the cone ERG in the central retina. The multifocal ERG results also demonstrated that the amplitude ratio of the positive wave to the a-wave was maximal in the central retina, and became gradually decreased towards the peripheral retina in a cCSNB patient and an APB-treated monkey supporting our combined findings of the full-field ERGs and focal macular cone ERGs. These results indicated that there is a unique spatial variation in the waveform of the cone ERGs. Other pharmacological studies in monkeys (Hare & Ton, 2002; Hood, Frishman, Saszik, & Viswanathan, 2002) also showed several spatial variations in the waveform of the cone ERGs using multifocal ERG technique, but they did not separate the on- and off-responses.

By adding PDA to APB, we found that the remaining positive wave of the cone ERG, which was seen even after blocking the cone on-pathway, originated from post-photoreceptor neurons which are sensitive to PDA, i.e., retinal neurons of the off-pathway or horizontal cells (Fig. 5). However, we could not identify exactly which retinal neurons/circuits contributed to this positive component. To identify the exact origin of this positive wave, further studies are needed using other pharmacological agents which affects specific retinal neurons.

Acknowledgments

The authors thank Laura J. Frishman of University of Huston for providing us her modified ophthalmoscope for multifocal ERG recordings for monkeys. We also thank Masao Yoshikawa, Eiichiro Nagasaka, Hidetaka Kudo of Mayo Corporation for technical helps.

References

Allen, L. E., Zito, I., Bradshaw, K., Patel, R. J., Bird, A. C., Fitzke, F., et al. (2003). Genotype-phenotype correlation in British families with X linked congenital stationary night blindness. *British Journal of Ophthalmology, 87*, 1413–1420.

Bech-Hansen, N. T., Naylor, M. J., Maybaum, T. A., Sparkes, R. L., Koop, B., Birch, D. G., et al. (2000). Mutations in NYX, encoding the leucine-rich proteoglycan nyctalopin, cause X-linked complete congenital stationary night blindness. *Nature Genetics, 26*, 319–323.

Dryja, T. P., McGee, T. L., Berson, E. L., Fishman, G. A., Sandberg, M. A., Alexander, K. R., et al. (2005). Night blindness and abnormal cone electroretinogram ON responses in patients with mutations in the GRM6 gene encoding mGluR6. *Proceedings of the National Academy of Sciences of the United States of America, 102*, 4884–4889.

Evers, H. U., & Gouras, P. (1986). Three cone mechanisms in the primate electroretinogram: Two with, one without OFF-center bipolar responses. *Vision Research, 26*, 245–254.

Hare, W. A., & Ton, H. (2002). Effects of APB, PDA, and TTX on ERG responses recorded using both multifocal and conventional methods in monkey. Effects of APB, PDA, and TTX on monkey ERG responses. *Documenta Ophthalmologica., 105*, 189–222.

Hood, D. C., Frishman, L. J., Saszik, S., & Viswanathan, S. (2002). Retinal origins of the primate multifocal ERG: Implications for the human response. *Investigative Ophthalmology & Visual Science, 43*, 1673–1685.

Houchin, K., Purple, R. L., & Wirtschafter, J. D. (1991). X-linked congenital stationary night blindness and depolarizing bipolar system dysfunction. [ARVO abstract]. *Investigative Ophthalmology & Visual Science, 32*, S1229 (Abstract No. 2741S).

Khan, N. W., Kondo, M., Hiriyanna, K. T., Jamison, J. A., Bush, R. A., & Sieving, P. A. (2005). Primate retinal signaling pathways: Suppressing ON-pathway activity in monkey with glutamate analogues mimics human CSNB1-NYX genetic night blindness. *Journal of Neurophysiology, 93*, 481–492.

Knapp, A. G., & Schiller, P. H. (1984). The contribution of on-bipolar cells to the electroretinogram of rabbits and monkeys. *Vision Research, 24*, 1841–1846.

Kondo, M., & Miyake, Y. (2000). Assessment of local cone on- and off-pathway function using multifocal ERG technique. *Documenta of Ophthalmologica, 100*, 139–154.

Kondo, M., Miyake, Y., Horiguchi, M., Suzuki, S., & Tanikawa, A. (1998). Recording multifocal electroretinogram on and off responses in humans. *Investigative Ophthalmology & Visual Science, 39*, 574–580.

Kondo, M., Miyake, Y., Kondo, N., Tanikawa, A., Suzuki, S., Horiguchi, M., et al. (2001). Multifocal ERG findings in complete type congenital stationary night blindness. *Investigative Ophthalmology & Visual Science, 42*, 1342–1348.

Kondo, M., Piao, C. H., Tanikawa, A., Horiguchi, M., Terasaki, H., & Miyake, Y. (2000). Amplitude decrease of photopic ERG b-wave at higher stimulus intensities in humans. *Japanese Journal of Ophthalmology, 44*, 20–28.

Leifert, D., Todorova, M. G., Prunte, C., & Palmowski-Wolfe, A. M. (2005). LED-generated multifocal ERG on- and off-responses in complete congenital stationary night blindness—A case report. *Documenta Ophthalmologica, 111*, 1–6.

Marmor, M. F., Hood, D. C., Keating, D., Kondo, M., Seeliger, M. W., & Miyake, Y. (2003). Guidelines for basic multifocal electroretinography (mfERG). *Documenta Ophthalmologica, 106*, 105–115.

Miyake, Y. (1988b). Studies of local macular ERG [in Japanese]. *Journal of Japanese Ophthalmological Society, 92*, 1418–1449.

Miyake, Y., Horiguchi, M., Suzuki, S., Kondo, M., & Tanikawa, A. (1997). Complete and incomplete type congenital stationary night blindness as a model of "OFF-retina" and "ON-retina". In M. M. LaVail, J. G. Hollyfield, & R. E. Anderson (Eds.), *Degenerative retinal diseases* (pp. 31–41). New York: Plenum Publishing.

Miyake, Y., Shiroyama, N., Ota, I., & Horiguchi, M. (1988a). Oscillatory potentials in electroretinograms of the human macular region. *Investigative Ophthalmology & Visual Science, 29*, 1631–1635.

Miyake, Y., Yagasaki, K., Horiguchi, M., & Kawase, Y. (1987). On- and off-responses in photopic electroretinogram in complete and incomplete types of congenital stationary night blindness. *Japanese Journal of Ophthalmology, 31*, 81–87.

Miyake, Y., Yagasaki, K., Horiguchi, M., Kawase, Y., & Kanda, T. (1986). Congenital stationary night blindness with negative electroretinogram: A new classification. *Archives of Ophthalmology, 104*, 1013–1020.

Pusch, C. M., Zeitz, C., Brandau, O., Pesch, K., Achatz, H., Feil, S., et al. (2000). The complete form of X-linked congenital stationary night blindness is caused by mutations in a gene encoding a leucine-rich repeat protein. *Nature Genetics, 26*, 324–327.

Rangaswamy, N. V., Hood, D. C., & Frishman, L. J. (2003). Regional variations in local contributions to the primate photopic flash ERG: Revealed using the slow-sequence mfERG. *Investigative Ophthalmology & Visual Science, 44*, 3233–3247.

Saeki, M., & Gouras, P. (1996). Cone ERGs to flash trains: The antagonism of a later flash. *Vision Research, 36*, 3229–3235.

Sieving, P. A., Murayama, K., & Naarendorp, F. (1994). Push-pull model of the primate photopic electroretinogram: a role for hyperpolarizing neurons in shaping the b-wave. *Visual Neuroscience, 11*, 519–532.

Terasaki, H., Miyake, Y., Nomura, R., Horiguchi, M., Suzuki, S., & Kondo, M. (1999). Blue-on-yellow perimetry in the complete type of congenital stationary night blindness. *Investigative Ophthalmology & Visual Science, 40*, 2761–2764.

Ueno, S., Kondo, M., Niwa, Y., Terasaki, H., & Miyake, Y. (2004). Luminance dependence of neural components that underlies the primate photopic electroretinogram. *Investigative Ophthalmology & Visual Science, 45*, 1033–1040.

Ueno, S., Kondo, M., Ueno, M., Miyata, K., Terasaki, H., & Miyake, Y. (2006). Contribution of retinal neurons to d-wave of primate photopic electroretinograms. *Vision Research, 46*, 658–664.

Young, R. S. L. (1991). Low-frequency component of the photopic ERG in patients with X-linked congenital stationary night blindness. *Clinical Vision Science, 6*, 309–315.

Young, R. S. L., Price, J., & Harrison, J. (1986). Psychophysical study of rod adaptation in patients with congenital stationary night blindness. *Clinical Vision Science, 1*, 137–143.

Recording Focal Macular Photopic Negative Response (PhNR) from Monkeys

Mineo Kondo, Yukihide Kurimoto, Takao Sakai, Toshiyuki Koyasu, Kentaro Miyata, Shinji Ueno, and Hiroko Terasaki

Purpose. To record the photopic negative response (PhNR) of the focal electroretinograms (ERGs) from the macula of monkeys and to study the properties of the focal macular PhNRs.

Methods. Focal macular ERGs were recorded from five rhesus monkeys using a modified infrared fundus camera, in which a red stimulus spot on a blue illuminated background were incorporated. The effects of different stimulus intensities and durations presented on a steady blue background of 100 scot cd/m^2 on the focal macular PhNRs were investigated. Focal macular PhNRs were also recorded before and after an intravitreous injection of tetrodotoxin (TTX).

Results. Focal ERG responses from a photocoagulated retinal site were recordable when the luminance of the red stimulus spot was ≤55 phot cd/m^2 and was presented on a steady blue background of 100 scot cd/m^2. The amplitude of the focal macular PhNR increased with increasing stimulus intensities and was larger than that of the b-wave at all stimulus intensities. The amplitude of the focal macular PhNR was largest at stimulus durations of 30 to 50 ms. An intravitreous injection of TTX essentially eliminated the focal macular PhNR.

Conclusions. It is possible to record focal macular PhNRs from monkeys by using a red stimulus spot on a blue background. Investigations of focal PhNRs can be a useful method of studying inner retinal function of local areas in normal and diseased retinas. (*Invest Ophthalmol Vis Sci.* 2008;49:3544–3550) DOI: 10.1167/iovs.08-1798

The photopic negative response (PhNR) is a slow, negative-going wave of the photopic electroretinogram (ERG) that appears immediately after the b-wave. This component was first identified by Viswanathan et al.[1] in 1999. They demonstrated that the PhNR was reduced in eyes of monkeys with increased intraocular pressure and reduced visual field sensitivity. In addition, they reported that the PhNR was essentially eliminated by an intravitreous injection of tetrodotoxin (TTX),[1–3] a selective blocker of voltage-gated Na^+ channels.[4–6] These results suggest that the PhNR originates mainly from the spiking activity of inner retinal neurons including the retinal ganglion cells and their axons.

In clinical studies, the PhNR has been reported to be reduced in patients with glaucoma,[7–9] optic nerve diseases,[10–12] and retinal vascular diseases that predominantly affect the inner retina.[13–15] We have reported that the amplitude of the PhNR is selectively reduced after macular hole surgery, indicating that there are some functional impairments in the inner retina after this type of surgery.[16] The results of these clinical studies suggest that recordings of the PhNR can provide a means for objective assessment of inner retinal function.

To date, the PhNR has been elicited mainly by full-field stimuli in both basic and clinical studies. However, the full-field ERG is the summed response from the entire retina, and it is difficult to assess the function of localized retinal areas by full-field ERGs. There are some reports on recording the PhNR from localized retinal areas,[2,7,17,18] but the characteristics of the focal PhNR in primates is less well understood. The focal PhNR is important because many diseases, including glaucoma and optic nerve diseases, affect selective areas of the retina. Therefore, we believed that developing a technique to record focal PhNRs could be useful for both basic research and clinical applications.

Thus, the purpose of this study was to determine whether a focal PhNR could be recorded from local areas of the monkey retina. For this, we developed a new recording system with a modified infrared fundus camera. A red stimulus spot was used on a blue illuminated background, because it has been reported recently that this color combination is most effective in eliciting large PhNRs especially at weak to moderate stimulus intensities.[3]

Methods

Stimulus and Observation Systems

Our new system for eliciting and recording focal PhNRs consisted of a modified infrared fundus camera and a stimulator that controlled the light-emitting diodes (LEDs) used for the stimulus and background illumination (Fig. 1A). An infrared television fundus camera (model VX-10; Kowa, Tokyo, Japan) was modified to obtain a Maxwellian stimulating system (Fig. 2). The image from this fundus camera was fed to a television monitor with a 45° view of the posterior pole of the eye (Fig. 1B). The position of the stimulus spot on the fundus was monitored on the television screen, and could be moved by the examiner with a joystick (Fig. 1A).

A red LED (λ_{max} = 627 nm; LXK2-PD12-S00; Philips Lumileds, San Jose, CA) was used as the stimulus source, and a blue LED (λ_{max} = 450 nm; L450, Epitex, Kyoto, Japan) was used for the background illumination that covered a retinal area of 45° (Fig. 2). The 15° red stimulus spot on the blue background that was photographed with a digital camera placed at the position of the monkey's eye is shown in Figure 1C. The size of the stimulus spot could be changed from 5° to 15°; the 15° stimulus spot was mainly used in this study.

The luminance of the blue background was fixed at 100 scot cd/m^2, which is known to be high enough to suppress the rod photoreceptors. The luminance of the red stimulus spot was increased from 2 to 204 phot cd/m^2, and the stimulus duration was increased from 5 to 150

From the Department of Ophthalmology, Nagoya University Graduate School of Medicine, Nagoya, Japan.

Supported by Health Sciences Research Grants (H16-sensory-001) from the Ministry of Health, Labor and Welfare, Japan, and by Grants 18591913 and 18390466 from the Ministry of Education, Culture, Sports, Science and Technology, Japan.

Submitted for publication January 27, 2008; revised March 29, 2008; accepted June 16, 2008.

Disclosure: **M. Kondo**, None; **Y. Kurimoto**, None; **T. Sakai**, None; **T. Koyasu**, None; **K. Miyata**, None; **S. Ueno**, None; **H. Terasaki**, None

The publication costs of this article were defrayed in part by page charge payment. This article must therefore be marked "*advertisement*" in accordance with 18 U.S.C. §1734 solely to indicate this fact.

Corresponding author: Mineo Kondo, Department of Ophthalmology, Nagoya University Graduate School of Medicine, 65 Tsuruma-cho, Showa-ku, Nagoya 466-8550, Japan; kondomi@med.nagoya-u.ac.jp.

Investigative Ophthalmology & Visual Science, August 2008, Vol. 49, No. 8

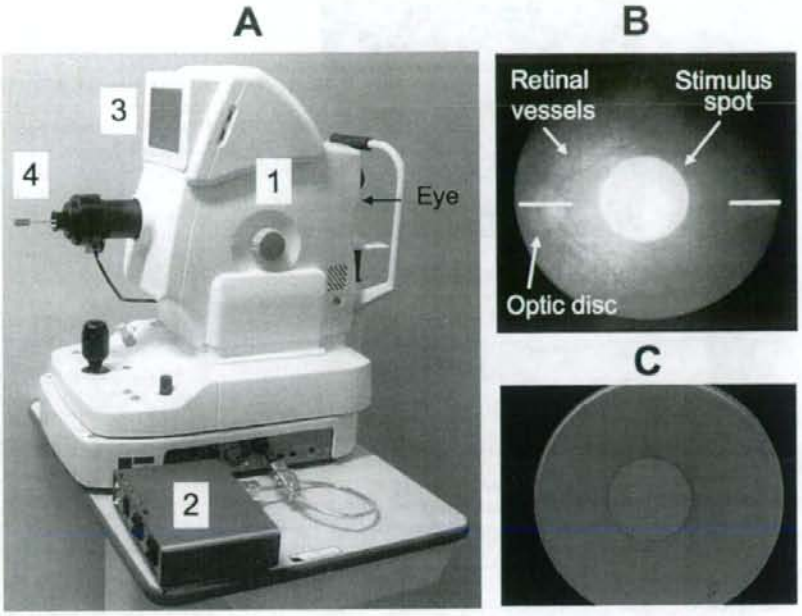

FIGURE 1. (A) Stimulus and observation system for recording the focal PhNR. This system consists of a modified infrared fundus camera (1) and LED control box (2). The infrared fundus image can be observed on a monitor (3), and the stimulus spot can be moved with a joystick (4). (B) Infrared fundus image of the monkey retina. A 15° stimulus spot positioned on the monkey's macula. (C) Image of the *red* stimulus spot on the *blue* background. This image was photographed by a digital camera at the position of the monkey's eye.

ms. The stimulus intensity was also expressed in energy units (i.e., phot cd-s/m^2, for brief flashes of ≤30 ms). The stimulus repetition rate was fixed at 2 Hz.

The luminances of the stimulus and background illumination were measured at the position of the corneal surface and then converted to the value at the retinal surface. These luminances were measured with a photometer (model IL 1700; International Light, Newburyport, MA).

Recording and Analyses

ERGs were recorded with a Burian-Allen bipolar contact lens electrode (Hansen Ophthalmic Development Laboratories, Iowa City, IA). The ground electrode was attached to the ipsilateral ear. The responses were amplified, and the band-pass filters were set at 0.5 to 1000 Hz. The ERGs were digitized at 5 kHz, and 100 to 300 responses were averaged for each recording (MEB-9100 Neuropack; Nihon Kohden, Tokyo, Japan).

The amplitude of the PhNR was measured from the baseline to the bottom of the negative trough after the b-wave for the brief flashes (≤ 30 ms), or was measured from the positive peak of the b-wave to the negative trough after the b-wave for the long-duration flashes (≥50 ms), as in previous studies.[1–3] The amplitudes of the a- and b-waves were measured from the baseline to the first negative trough and from the negative trough to the next positive peak, respectively.

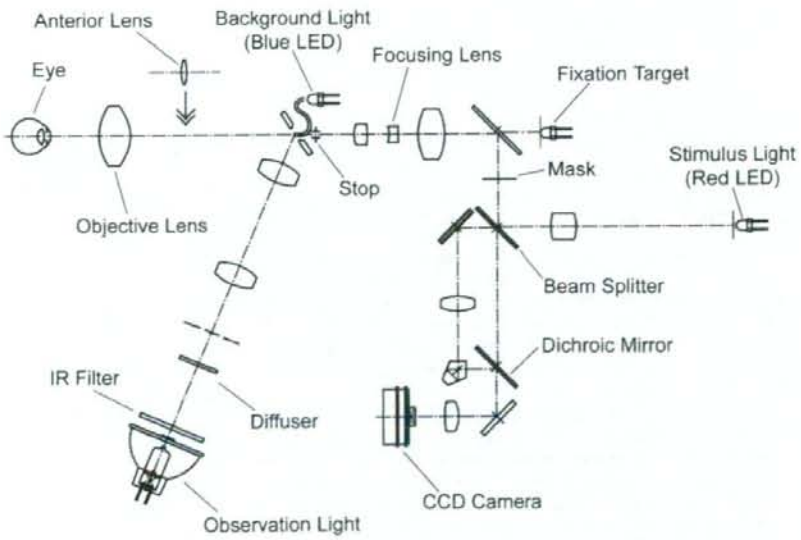

FIGURE 2. Diagram of the focal PhNR recording system with fundus monitoring with an infrared fundus camera. A red LED was used for the stimulus source, and a blue LED was used for the background illumination.

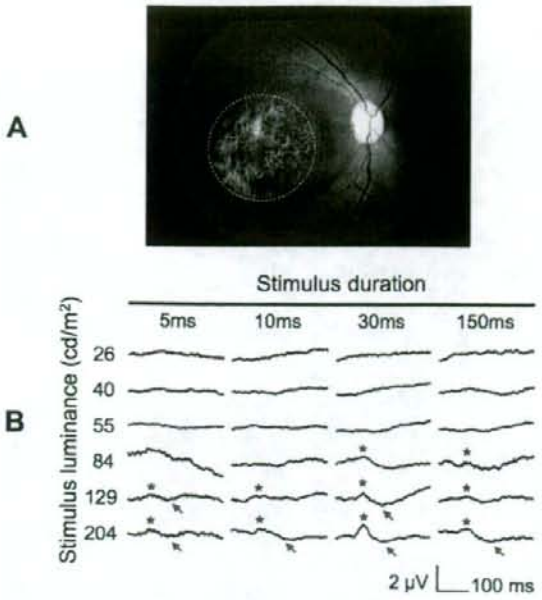

FIGURE 3. Studies of stray light effect in our system. (**A**) Fundus photograph of a monkey whose macula was damaged by 15° in the central area by focal laser photocoagulation (within the *white dashed line*). (**B**) Focal ERGs recorded with a 15° stimulus spot centered on the photocoagulation. Stimulus luminance and stimulus duration were changed on a steady blue background illumination of 100 scot cd/m^2. Small positive (*red asterisks*) or negative (*blue arrows*) waves were detected when the stimulus luminance was 84 cd/m^2 or higher, presumably due to the effect of stray light.

Animals

Five eyes of five rhesus monkeys (*Macaca mulatta*) were studied. The animals were sedated with an intramuscular injection of ketamine hydrochloride (7 mg/kg initial dose; 5 to 10 mg/kg/h maintenance dose) and xylazine (0.6 mg/kg). The respiration and heart rate were monitored, and hydration was maintained with slow infusion of lactated Ringer solution. The cornea was anesthetized with topical 1% tetracaine, and the pupils dilated with topical 0.5% tropicamide, 0.5% phenylephrine HCl, and 1% atropine. All experimental and animal care procedures adhered to the ARVO Statement for the Use of Animals in Ophthalmic and Vision Research and were approved by the Institutional Animal Care Committee of the Nagoya University.

Drug Application

The drugs and intravitreous injection techniques have been described in detail.[1-3,17,19,20] The drugs were injected into the vitreous with a 30-gauge needle inserted through the pars plana approximately 3 mm posterior to the limbus. TTX (Kanto Chemical, Tokyo Japan) was dissolved in sterile saline, and 0.05 to 0.07 mL was injected. The intravitreous concentration of TTX was 4 μM, assuming that the monkey's vitreous volume is 2.1 mL.

Because the TTX effect reaches its maximum at approximately 60 minutes after the drug injection, recordings were begun approximately 60 to 90 minutes after the injections, and studies were completed within 3 hours. Although the effects of these drugs are mostly reversible after a recovery period of several weeks, the results that are shown were recorded from eyes not previously treated.

RESULTS

Effects of Stray Light

To determine that the PhNRs we recorded were indeed focal responses, we investigated the effect of stray light on the responses with our system. First, we recorded focal ERGs using a 5° stimulus spot placed on the optic nerve head of monkeys. Different stimulus luminances (2–204 phot cd/m^2) and stimulus durations (5, 10, 30, and 150 ms) were presented on a steady blue background illumination of 100 scot cd/m^2. There were no detectable ERG responses (<0.4 μV) when the stimulus luminance was ≤55 phot cd/m^2 for all stimulus durations. A small positive or negative response was elicited by a stimulus luminance of 84 phot cd/m^2 and stimulus durations of 30 and 150 ms. The amplitudes of the response increased with increasing stimulus luminance (data not shown).

We next examined the stray light effect by recording focal ERGs 1 month after an argon laser photocoagulation of a 15° spot in the macular area (Fig. 3A). ERGs were elicited by stimulating the photocoagulated area with different stimulus luminances (26–204 phot cd/m^2), stimulus durations (5, 10, 30, and 150 ms), and a 15° stimulus spot. The stimulus spot was presented on a steady blue background illumination of 100 scot cd/m^2 in one monkey. We found that the response amplitudes were lower than the noise level (< 0.4 μV) when the stimulus luminance was ≤55 phot cd/m^2 for all stimulus durations. A small positive wave (Fig. 3B, red asterisks) or negative wave (blue arrows) was recorded when the stimulus luminance was ≥84 phot cd/m^2. These small responses were more prominent at stimulus durations of 30 and 150 ms and were most likely due to stray light, because the central retina within 15° had been completely photocoagulated.

Based on these results, we concluded that stimulus luminances of ≤55 phot cd/m^2 presented on a steady blue background of 100 scot cd/m^2 are the optimal stimulus for eliciting focal ERGs in our system.

Effect of Stimulus Intensity

Representative focal macular ERGs elicited by stimulus luminances of 2 to 55 phot cd/m^2 for four stimulus durations of 5, 10, 30, and 150 ms are shown in Figure 4. It is clear that the amplitude of the focal PhNRs increased with increasing stimulus luminance for all stimulus durations.

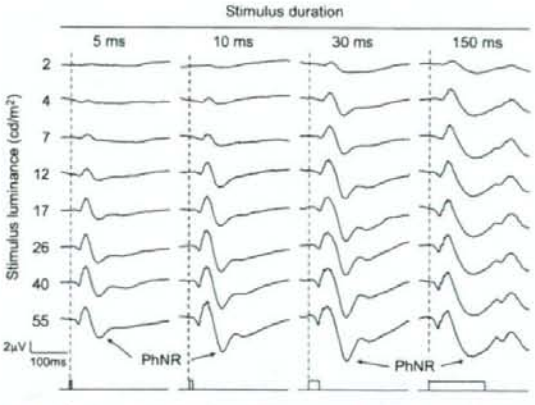

FIGURE 4. Representative focal ERGs elicited from a rhesus monkey by different stimulus luminances (2–55 phot cd/m^2) and different stimulus durations (5, 10, 30, and 150 ms). The amplitude of PhNR increases with increasing stimulus luminances.

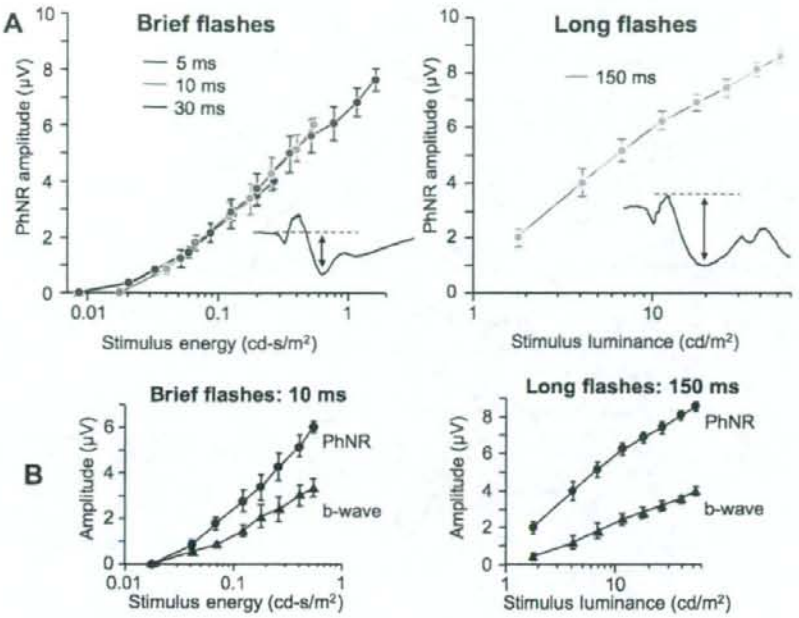

FIGURE 5. (A) Stimulus intensity-response curves of the mean (± SEM, $n = 4$) amplitudes of the focal macular PhNR. The PhNR amplitudes are plotted as a function of stimulus energy (cd-s/m^2) for brief flashes of 5 to 30 ms in the left half and are plotted as a function of stimulus luminance (cd/m^2) for a long 150-ms flash in the right half. (B) Comparison of stimulus intensity-response curves of the mean (± SEM, $n = 4$) amplitudes of the b-wave and PhNR for stimulus duration of 10 ms (*left*) and 150 ms (*right*).

The relationship between the stimulus intensities and the average amplitudes of the focal macular PhNRs is shown in Figure 5A. The amplitudes of the focal macular PhNR are plotted as a function of stimulus energy for brief flashes (5, 10, and 30 ms, left), and are plotted as a function of stimulus luminance for long flashes (150 ms, right). We found that when the stimulus duration was shorter than the integration time of PhNR (≤ 30 ms), the amplitude of the focal macular ERG was dependent on the stimulus energy (Fig. 5A).

One of the interesting findings was that the amplitude of PhNR was larger than that of the b-wave for all stimulus intensities and was more than double the b-wave amplitude at a stimulus duration of 150 ms at all stimulus luminances (Fig. 5B).

Effect of Stimulus Duration

We also examined the effects of stimulus duration on the focal macular PhNR of monkeys. Representative focal macular ERGs elicited by different stimulus durations of 5 to 150 ms at a constant stimulus luminance of 55 phot cd/m^2 are shown in Figure 6A. The stimulus energy (phot cd-s/m^2) is also indicated for the brief flashes of ≤30 ms.

The amplitude of the focal macular PhNR increased with increasing stimulus durations when the stimulus durations were shorter than 30 to 50 ms. This increase in the amplitude is most likely due to the increase in the stimulus energy (see also Fig. 5A). Further increases in the stimulus duration led to a slight decrease in the PhNR amplitude (Fig. 6B).

We also found that the implicit time of the PhNR was dependent on the stimulus duration. The implicit time of the PhNR was approximately 75 ms for a stimulus of 5 ms duration and became longer with increasing stimulus durations and then reached a maximum implicit time (110 ms) at approximately 50 ms duration (Fig. 6A, red dashed vertical lines). This gradual increase in the implicit time of the PhNR most likely resulted from an increase in stimulus energy and the increase in the midpoint of the stimulus. Further increases in the stimulus duration did not change the implicit time of the PhNR.

We also found that another slow negative response (Fig. 6A, asterisks) developed after the stimulus offset for longer stimulus durations of 100 to 150 ms. This negative response was thought to be a homologue of the PhNR to the stimulus offset (PhNR$_{Off}$), which has been reported in studies of full-field photopic ERGs.[1–3,20]

Effect of Intravitreous Injection of TTX

Finally, we studied whether the focal macular PhNR recorded from monkeys changed after an intravitreous injection of TTX, which blocks voltage-gated sodium channels and prevents the generation of sodium-based action potentials. Representative waveforms of focal macular ERGs recorded before (black) and after (red) an intravitreous injection of TTX are shown in Figure 7. The stimulus luminance was set at 55 phot cd/m^2, and the responses to stimulus durations of 5 to 150 ms are shown. We found that blocking the spiking activities of inner retinal neurons by TTX essentially eliminated the focal macular PhNR, which was similar to the effect of TTX on the full-field photopic ERG.[1–3]

For long-duration stimuli of 100 to 150 ms, the slow negative potential that was found after the light offset (PhNR$_{off}$, Fig. 7, asterisks) was also not present after TTX. Similar effects have been reported for full-field ERG studies.[1–3,20]

Although the major effect of TTX was seen in the PhNR, other ERG components of the focal macular ERG were also slightly altered after TTX. The amplitude of the a-wave became slightly smaller, and the implicit times of the b-wave were delayed. These minor changes were also very similar to those reported for full-field PhNR studies.[1–3]

Discussion

Our results showed that focal PhNRs can be recorded from the macular area of monkeys by using our newly developed system. In this system, a red stimulus spot was presented on a blue background, which was earlier shown to be the optimal stim-

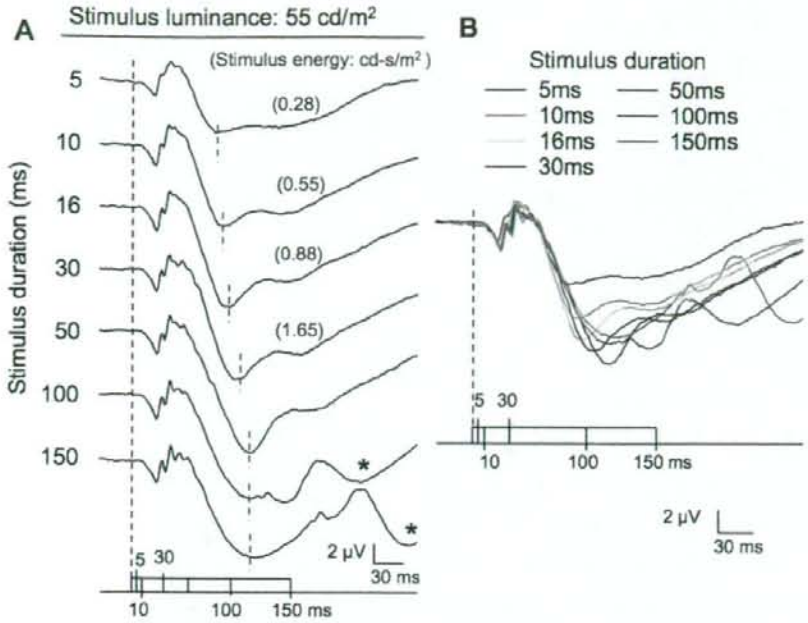

FIGURE 6. Effect of stimulus duration on the focal PhNR. (A) Representative focal ERGs elicited by different stimulus durations (5–150 ms) for a constant stimulus luminance of 55 phot cd/m². *Vertical dotted line*: peak of the PhNR. The values of stimulus energy (cd-s/m²) are also indicated for brief flashes of 5 to 30 ms. (B) Superimposed focal ERG waveforms recorded with different stimulus durations (5–150 ms). Stimulus luminance was fixed at 55 phot cd/m².

ulus conditions to elicit large PhNRs especially at low to intermediate stimulus intensities.[3] In addition, our system allowed us to monitor the position of the stimulus spot on the monkey's fundus during the recordings. Our ability to record focal PhNRs from monkey eyes is important, because this will allow us to manipulate the recording conditions or alter the normal PhNR with drugs known to affect specific neural elements to study the physiological properties of the PhNRs.

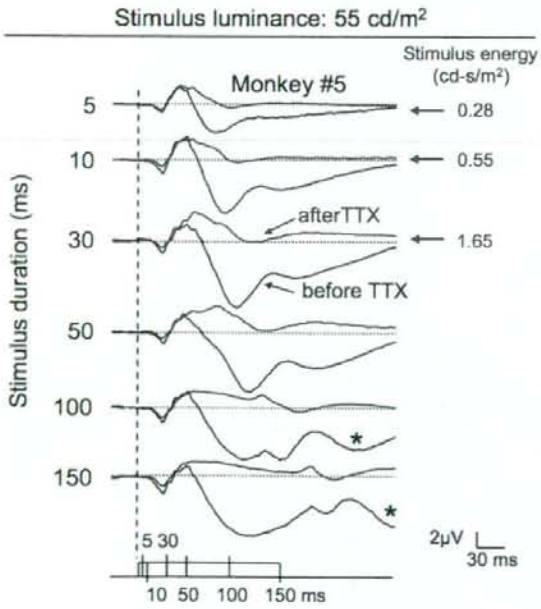

FIGURE 7. Focal ERGs before and after intravitreous injection of TTX in one monkey. The focal ERGs before (*black lines*) and after TTX (*red lines*) are superimposed. Stimulus luminance was fixed at 55 phot cd/m², and stimulus duration was changed from 5 to 150 ms. Note that the amplitude of focal PhNR was greatly reduced after TTX. The other slow negative response to the stimulus offset ($PhNR_{Off}$, asterisks) was also reduced after TTX.

To establish a technique to record focal ERGs, it was important for us to determine the optimal combination of stimulus and background intensities.[21–28] Based on the results of trying to elicit focal ERGs from the optic nerve head and from a retinal site damaged by focal laser coagulation, we found that a 15° red stimulus spot of ≤55 phot cd/m² presented on a steady blue background of 100 scot cd/m², will elicit a focal ERG. For stimulus intensities >55 phot cd/m², small responses were recorded even from the retinal site damaged by focal laser coagulation, and this response was most likely due to stray light (Fig. 3). The stray light effect was dependent on the stimulus intensity and was greater for longer stimulus durations of 30 and 150 ms (Fig. 3B).

We studied the response characteristics of the focal macular PhNRs recorded by our system, and found the following: (1) The focal macular PhNR was a slow, negative response, with an implicit time of approximately 75 ms for short-duration stimuli and approximately 110 ms for long-duration stimuli (Fig. 6); (2) for long-duration stimuli, the PhNR was seen after both the onset and the offset of the stimulus (Figs. 4, 6); (3) the amplitude of the focal macular PhNR increased with increasing stimulus intensity (Fig. 5); and, (4) the amplitude of the focal macular PhNR was greatly reduced after an intravitreous injection of TTX.

These results showed that the response characteristics of focal PhNRs recorded from the monkey's macula were very similar to those of the full-field PhNR,[1–3,11] and that this negative response originates mainly from the action potentials of the inner retinal neurons.

One interesting finding in our study was that the amplitudes of focal macular PhNRs recorded by our system were large; the maximum PhNR amplitude reached 6.1 μV for a 10-ms

duration stimulus and 8.3 μV for a 150-ms duration stimulus. The amplitudes of the focal PhNR recorded from the 15° macular area were relatively large when compared with the amplitudes of the full-field PhNR which were 25 to 40 μV in earlier monkey studies.[1–3,11] Large PhNR amplitudes in our focal ERGs can also be understood when one examines the amplitude of the b-wave and PhNR. The amplitude of PhNR was larger than that of the b-wave in all stimulus conditions and was more than twice that of the b-wave for long-duration stimuli of 150 ms (Fig. 5B).

The reason for the relatively large PhNR amplitude in the macular region in monkeys was not examined, but may be explained by two possibilities. First, the density of ganglion cells (number/mm^2) is highest in the central retina of monkeys,[29–33] and the slope of ganglion cell number as a function of retinal eccentricity is steeper than that of cone cells in the human retina.[34] This high ganglion cell density in the central retina may contribute to the large amplitude of the macular PhNR. And second, we used a red stimulus spot on a blue background. This combination was recently shown to be optimal for eliciting maximum PhNR amplitude. Using various stimulus and background color combinations, Rangaswamy et al.[5] concluded that at weak to moderate stimulus intensities, the amplitude of PhNR is larger in response to stimuli that are relatively more cone specific.

The amplitude of macular PhNR increased with increasing stimulus durations up to 30 to 50 ms, because of due to the increase in the stimulus energy. However, further increases in the stimulus duration led to a decrease in amplitude. The decrease in amplitude may be explained by the separation of the two PhNR components: $PhNR_{on}$ elicited by stimulus onset and $PhNR_{off}$ elicited by stimulus offset, both of which are superimposed when a brief-flash stimuli (≤50 ms) is used. A second possibility is that this amplitude decrease may be due to factors other than the spiking activities of inner retinal neurons. As seen in Figure 7, the longer duration stimuli tended to elicit prolonged b-waves (plateau) when the PhNR was eliminated by TTX, whereas the brief-flash responses generally leveled off at the baseline.

There remain some critical matters that should be addressed in future studies. First, we did not show how full-field PhNR and focal macular PhNR are different with regard to the intensity–response function, duration–response function, and the effect of TTX. To determine these differences, we must compare the full-field and focal PhNRs in the same stimulus and recording conditions. Second, although we succeeded in recording focal PhNRs from the macula of monkeys, we did not examine whether there are any regional variations across the retina in the waveform or amplitude of the PhNR. We are currently comparing the focal PhNRs between upper and lower retinas, or nasal and temporal retinas by using semicircular stimulus spots. Finally, in this study we used only one type of electrode, the Burian-Allen bipolar contact lens electrode. However, it is known that the speculum of this electrode, which also acts as the reference, can pick up signals that can cancel out the signals picked up by the corneal electrode. It may be better to place the reference farther from the recording electrode (e.g., fellow eye), to maximize the response of small signals.[35,36]

In conclusion, we successfully recorded focal PhNRs from the macula of monkeys by using a red stimulus spot on a blue background. Although there are still many factors that need to be tested, we believe that examinations of the focal PhNRs can be a useful technique for studying the inner retinal function of local retinal areas in normal and diseased retinas.

Acknowledgments

The authors thank Yozo Miyake of Shukutoku University and Duco I. Hamasaki for discussions on the manuscript, and Masao Yoshikawa, Hideteka Kudo, and Ei-ichiro Nagasaka of Mayo Corporation for technical assistance.

References

1. Viswanathan S, Frishman LJ, Robson JG, et al. The photopic negative response of the macaque electroretinogram: reduction by experimental glaucoma. *Invest Ophthalmol Vis Sci*. 1999;40:1124–1136.
2. Viswanathan S, Frishman LJ, Robson JG. The uniform field and pattern ERG in macaques with experimental glaucoma: removal of spiking activity. *Invest Ophthalmol Vis Sci*. 2000;41:2797–2810.
3. Rangaswamy NV, Shirato S, Kaneko M, et al. Effects of spectral characteristics of Ganzfeld stimuli on the photopic negative response (PhNR) of the ERG. *Invest Ophthalmol Vis Sci*. 2007;48:4818–4828.
4. Narahashi T, Moore JW, Scott WR. Tetrodotoxin blockage of sodium conductance increase in lobster giant axons. *J Gen Physiol*. 1964;47:965–974.
5. Bloomfield SA. Effect of spike blockade on the receptive-field size of amacrine and ganglion cells in the rabbit retina. *J Neurophysiol*. 1996;75:1878–1893.
6. Stafford DK, Dacey DM. Physiology of the A1 amacrine: a spiking, axon-bearing interneuron of the macaque monkey retina. *Vis Neurosci*. 1997;14:507–522.
7. Colotto A, Falsini B, Salgarello T, et al. Photopic negative response of the human ERG: Losses associated with glaucomatous damage. *Invest Ophthalmol Vis Sci*. 2000;41:2205–2211.
8. Viswanathan S, Frishman LJ, Robson JG, et al. The photopic negative response of the flash electroretinogram in primary open angle glaucoma. *Invest Ophthalmol Vis Sci*. 2001;42:514–522.
9. Drasdo N, Aldebasi YH, Chiti Z, et al. The S-cone PhNR and pattern ERG in primary open angle glaucoma. *Invest Ophthalmol Vis Sci*. 2001;42:1266–1272.
10. Gotoh Y, Machida S, Tazawa Y. Selective loss of the photopic negative response in patients with optic nerve atrophy. *Arch Ophthalmol*. 2004;122:341–346.
11. Rangaswamy NV, Frishman LJ, Dorotheo EU, et al. Photopic ERGs in patients with optic neuropathies: comparison with primate ERGs after pharmacologic blockade of inner retina. *Invest Ophthalmol Vis Sci*. 2004;45:3827–3837.
12. Miyata K, Nakamura M, Kondo M, et al. Reduction of oscillatory potentials and photopic negative response in patients with autosomal dominant optic atrophy with OPA1 mutations. *Invest Ophthalmol Vis Sci*. 2007;48:820–824.
13. Machida S, Gotoh Y, Tanaka M, Tazawa Y. Predominant loss of the photopic negative response in central retinal artery occlusion. *Am J Ophthalmol*. 2004;137:938–940.
14. Kizawa J, Machida S, Kobayashi T, et al. Changes of oscillatory potentials and photopic negative response in patients with early diabetic retinopathy. *Jpn J Ophthalmol*. 2006;50:367–373.
15. Chen H, Wu D, Huang S, Yan H. The photopic negative response of the flash electroretinogram in retinal vein occlusion. *Doc Ophthalmol*. 2006;113:53–59.
16. Ueno S, Kondo M, Piao CH, et al. Selective amplitude reduction of the PhNR after macular hole surgery: ganglion cell damage related to ICG-assisted ILM peeling and gas tamponade. *Invest Ophthalmol Vis Sci*. 2006;47:3545–3549.
17. Rangaswamy NV, Hood DC, Frishman LJ. Regional variations in local contributions to the primate photopic flash ERG: revealed using the slow-sequence mfERG. *Invest Ophthalmol Vis Sci*. 2003;44:3233–3247.
18. Fortune B, Wang L, Bui BV, et al. Local ganglion cell contributions to the macaque electroretinogram revealed by experimental nerve fiber layer bundle defect. *Invest Ophthalmol Vis Sci*. 2003;44:4567–4579.
19. Ueno S, Kondo M, Niwa Y, et al. Luminance dependence of neural components that underlies the primate photopic electroretinogram. *Invest Ophthalmol Vis Sci*. 2004;45:1033–1040.

20. Ueno S, Kondo M, Ueno M, et al. Contribution of retinal neurons to d-wave of primate photopic electroretinograms. *Vision Res*. 2006;46:658–664.
21. Brindley GS, Westheimer G. The spatial properties of the human electroretinogram. *J Physiol*. 1965;179:518–537.
22. Aiba TS, Alpern M, Maaseidvaag F. The electroretinogram evoked by the excitation of human foveal cones. *J Physiol*. 1967;189:43–62.
23. Jacobson JH, Kawasaki K, Hirose T. The human electroretinogram and occipital potential in response to focal illumination of the retina. *Invest Ophthalmol*. 1969;8:545–556.
24. Biersdorf WR, Diller DA. Local electroretinogram in macular degeneration. *Am J Ophthalmol*. 1969;68:296–303.
25. Hirose T, Miyake Y, Hara A. Simultaneous recording of electroretinogram and visual evoked response: focal stimulation under direct observation. *Arch Ophthalmol*. 1977;95:1205–1208.
26. Sandberg MA, Ariel M. A hand-held, two-channel stimulator-ophthalmoscope. *Arch Ophthalmol*. 1977;95:1881–1882.
27. Seiple WH, Siegel IM, Carr RE, Mayron C. Evaluating macular function using the focal ERG. *Invest Ophthalmol Vis Sci*. 1986;27:1123–1130.
28. Miyake Y, Shiroyama N, Horiguchi M, Ota I. Asymmetry of focal ERG in human macular region. *Invest Ophthalmol Vis Sci*. 1989;30:1743–1749.
29. Rolls ET, Cowey A. Topography of the retina and striate cortex and its relationship to visual acuity in rhesus monkeys and squirrel monkeys. *Exp Brain Res*. 1970;10:298–310.
30. Webb SV, Kaas JH. The sizes and distribution of ganglion cells in the retina of the owl monkey Aotus trivirgatus. *Vision Res*. 1976;16:1247–1254.
31. DeBruyn EJ, Wise VL, Casagrande VA. The size and topographic arrangement of retinal ganglion cells in the galago. *Vision Res*. 1980;20:315–327.
32. Stone J, Johnston E. The topography of primate retina: a study of the human, bushbaby, and new- and old-world monkeys. *J Comp Neurol*. 1981;196:205–224.
33. Perry VH, Cowey A. The ganglion cell and cone distributions in the monkey's retina: implications for central magnification factors. *Vision Res*. 1985;25:1795–1810.
34. Curcio CA, Allen KA. Topography of ganglion cells in human retina. *J Comp Neurol*. 1990;300:5–25.
35. Sutter EE, Bearse MA Jr. The optic nerve head component of the human ERG. *Vision Res*. 1999;39:419–436.
36. Hood DC, Bearse MA Jr, Sutter EE, et al. The optic nerve head component of the monkey's (Macaca mulatta) multifocal electroretinogram (mERG). *Vision Res*. 2001;41:2029–2041.

Correlation between Macular Volume and Focal Macular Electroretinogram in Patients with Retinitis Pigmentosa

Tadasu Sugita, Mineo Kondo, Chang-Hua Piao, Yasuki Ito, and Hiroko Terasaki

Purpose. To determine whether a significant correlation exists between the morphology of the macula measured by optical coherence tomography (OCT) and the amplitude of focal macular electroretinograms (fmERGs) in patients with retinitis pigmentosa (RP).

Methods. fmERGs were recorded in 43 patients with RP and 43 age-similar normal subjects, with a 15° stimulus spot, 5.6 to 5.8 mm in diameter on the fundus. The sum of the volume of the neural retina in the central 6 mm (total macular volume) was measured with the OCT system. The length of the photoreceptor inner segment/outer segment junction (IS/OS line) in a 6-mm diameter macular area was also measured in the OCT images.

Results. There was a weak correlation between the total macular volume and the fmERG amplitudes (correlation coefficient, 0.46 for the a-wave and 0.54 for the b-wave). The fmERG amplitudes in the patients with RP with IS/OS line longer than 2 mm were significantly larger than those in patients with RP with IS/OS line shorter than 2 mm, but the correlations between these two factors were weak. One major reason for the low correlations between the macular morphology and fmERGs was that there were some patients with RP who had normal macular volume and long IS/OS line, but had severely reduced focal macular ERGs.

Conclusions. Although the macular volume and length of the IS/OS line correlated weakly with the amplitude of the fmERGs, a preserved macular morphology does not necessarily guarantee normal-amplitude fmERGs in patients with RP. (*Invest Ophthalmol Vis Sci.* 2008;49:3551–3558) DOI:10.1167/iovs.08-1954

Retinitis pigmentosa (RP) is a subset of inherited retinal diseases characterized by a progressive loss of the rod and cone photoreceptors.[1–5] Past histopathologic studies on patients with RP[6–8] have shown that the earliest anatomic change is a shortening or distortion of the rod and cone photoreceptor outer segments. This change is followed by the loss of rod and cone photoreceptors beginning in the periphery and progressing toward the central retina.

It is important to evaluate the functional and structural changes in the macular area of patients with RP because the central retina is relatively better preserved until the late stages, and various subjective and objective examinations have been used. Focal ERGs[9–13] and multifocal ERGs[14–21] have been used to assess the macular function of eyes with RP, because these techniques can examine the neural activities of the macular area objectively.

Optical coherence tomography (OCT) is a noninvasive technique that can assess the morphology of the retina, especially the macula in vivo. This technique is especially useful in patients with RP, because OCT enables the investigator to evaluate the morphologic changes in each retinal layer and the overall retina.[22–36] It has been shown that the OCT-determined cross-sectional retinal images were well-correlated with retinal histology in animal models of retinal degeneration.[37–40] In addition, there is evidence that the OCT-determined structural changes in the central retina correlate with subjective visual functions including the visual acuity and visual threshold in patients with RP.[27,30,34,36] However, there is only one report on the relationship between the morphologic changes measured by OCT and macular function measured by focal macular ERGs (fmERGs) in patients with RP.[25] The relationship between the macular morphology and function in patients with RP can provide important information on the treatment of patients with retinal degeneration.[29,31–33]

Thus, the purpose of this study was to determine whether a significant correlation exists between the amplitude of the fmERGs and the sum of the volume of the neural retina in the central 6 mm of the macula (total macular volume) or the length of the photoreceptor inner/outer segment junction (IS/OS line) measured by OCT images in patients with typical retinitis pigmentosa (RP).

Methods

Subjects

This prospective study included 124 consecutive patients with RP who visited one ophthalmologist (MK) in the Department of Ophthalmology, Nagoya University Hospital, from January to December in 2006. The clinical diagnosis of RP was based on the ocular history, funduscopic findings, visual fields, and ISCEV (International Society for Clinical Electrophysiology of Vision) standard full-field ERGs.[41] The inclusion criteria were a diagnosis of RP with a complete medical examination, including best corrected visual acuity (BCVA) measured by the standard Japanese decimal visual acuity chart, fundus examination, Goldmann kinetic visual fields, full-field ERGs; BCVA had to be ≥0.3. The exclusion criteria were atypical RP (e.g., central RP, sector RP, or unilateral RP), opacities in the media including cataracts, and cystoid macular edema identified by the OCT. Based on these inclusion and exclusion criteria, 43 eyes of 43 patients with RP (19 males, 24 females; mean age, 41.7 years; range, 16–66) were analyzed. If both eyes met these criteria, then the data from only the right eye were used for the analyses.

The inheritance pattern was autosomal dominant in 6 (14%) patients, autosomal recessive in 6 (14%), and sporadic in 31 (72%). None of the patients was found to have X-linked RP. The best corrected visual acuity ranged from 0.3 to 1.2, and the mean logarithm of the minimum angle of resolution (logMAR) was 0.052 units.

For controls, fmERGs and OCT were recorded from 43 age-similar normal subjects (14 males, 29 females; mean age, 42.7 years, range,

From the Department of Ophthalmology, Nagoya University Graduate School of Medicine, Nagoya, Japan.

Supported by Grants-in Aid 18591913 (MK), 19500416 (YI), and 18390466 (HT) from the Ministry of Education, Culture, Sports, Science and Technology.

Submitted for publication February 29, 2008; revised April 13, 2008; accepted June 16, 2008.

Disclosure: **T. Sugita**, None; **M. Kondo**, None; **C.-H. Piao**, None, **Y. Ito**, None; **H. Terasaki**, None

The publication costs of this article were defrayed in part by page charge payment. This article must therefore be marked "*advertisement*" in accordance with 18 U.S.C. §1734 solely to indicate this fact.

Corresponding author: Mineo Kondo, Department of Ophthalmology, Nagoya University Graduate School of Medicine, 65 Tsuruma-cho, Showa-ku, Nagoya 466-8550, Japan; kondomi@med.nagoya-u.ac.jp.

16–67). None had known abnormalities of the visual system, and their visual acuity was ≥1.0 in all.

The research was conducted in accordance with the Institutional Guidelines of Nagoya University and conformed to the tenets of the World Medical Association's Declaration of Helsinki. Informed consent was obtained from each of the patients after they were provided sufficient information on the procedures to be used.

Focal Macular ERGs

The stimulus and recording systems used to record fmERGs have been described in detail.[15,42,43] Briefly, an infrared fundus camera equipped with a stimulus light, background illumination, and fixation target was used. The image from the camera was fed to a television monitor, and the examiner used the image on the monitor to maintain the stimulus on the macula. A stimulus spot size of 15° was selected because ocular biometry[44–46] has shown that a 15° stimulus spot covers a retinal area of 5.5 to 5.8 mm, which is approximately the size of the OCT-determined macular diameter (6.0 mm). The background light subtended a visual angle of 45°, and additional background illumination outside the central 45° produced a homogeneous background for nearly the entire visual field. The luminances of the white stimulus light and background light were 29.46 and 2.89 cd/m^2, respectively. Although this luminance of background light was not strong enough to suppress all the rod activity, we have shown that the fmERGs elicited by this method are generated mainly by the cone system, and the responses elicited by spot stimuli of 5 to 15° are local responses.[42,43]

A Burian-Allen bipolar contact lens electrode was used to record the fmERGs. This contact lens electrode system had low electrical noise and permitted a clear view of the fundus by the camera during the recordings. After the pupils were fully dilated with 0.5% tropicamide and 0.5% phenylephrine hydrochloride, fmERGs were elicited by a flicker train consisting of a square waves presented at 5 Hz (100-ms on and 100-ms off). Then, a series of 512 responses were averaged in a single cycle by a signal processor. The time constant of the bioamplifier was set at 0.03 seconds with a 100-Hz high-cut filter to record the a- and b-waves.

The amplitude of the a-wave was measured from the baseline to the first negative trough, and the amplitude of b-wave was measured from the trough of the a-wave to the positive peak of the b-wave.

OCT Measurements

The morphology of the macula was evaluated by a high-resolution optical coherence tomograph (Stratus model 3000, software ver. 4.0.1; Carl Zeiss Meditec, AG, Oberkochen, Germany). After the patients' pupils were fully dilated with 0.5% tropicamide and 0.5% phenylephrine, the sum of the volume of the neural retina in the central 6 mm of the macula (total macular volume) was measured using six scans of 6 mm in a radial pattern intersecting at the fixation point.

It is known that the automatic fast macular thickness map (FMTM) protocol often fails to identify the outer borders of the neural retina, which can lead to recording of erroneous retinal thicknesses and volumes.[47] Therefore, we used a program developed in our laboratory (Ishikawa K, et al. *IOVS* 2005;46:ARVO E-Abstract 1550),[48] by which the total macular volume was measured more precisely than that calculated by the conventional FMTM system. In this program, the user was able to set 20 cursors above and below a selected area manually. The inner cursors were set on the internal limiting membrane (ILM), and the outer cursors were set on the retinal pigment epithelium (RPE)–choriocapillaris hyperreflective complex borderline. Another set of cursors was set on the fovea of the OCT images. Then, each OCT radial scan was analyzed as a retinal map, and the total macular volume was calculated precisely by our software.

Past studies with the Stratus OCT and ultrahigh-resolution OCT demonstrated that there are two well-defined, parallel, highly reflective lines (HRLs) in the outer retinal layer.[49,50] It has been shown that the inner HRL corresponds to the photoreceptor inner/outer segment junction or the IS/OS line, and the outer HRL corresponds to the retinal pigment epithelium and choriocapillaris complex. To asses the relationship between the morphologic changes in the photoreceptor layer and the amplitude of the fmERGs, we classified the IS/OS line in patients with RP into three types: type 1, distinct IS/OS line longer than the central 2 mm; type 2, distinct IS/OS line only within the central 2 mm; and type 3, absence of IS/OS line within the central 6 mm (Fig. 1). To perform this classification, we reviewed the six tomographic images of each eye on a gray scale with an alignment image protocol, because the IS/OS line is more clearly visible on gray-scale tomographic images.[51] The classification was performed by TS in a masked manner.

Statistical Analyses

The significance of the differences between the patients with RP and normal control subjects was determined by nonparametric Mann-Whitney U tests. The correlations between the macular volume and the fmERG amplitudes were determined by the Spearman's rank correlation. Differences in the amplitudes among the three groups (types 1, 2, and 3) based on the length of the IS/OS line were analyzed with the nonparametric Kruskal-Wallis test and Scheffé's test, as the multiple comparison procedures. Differences and correlations were considered to be significant when $P < 0.05$.

Results

Representative OCT images and fmERGs recorded from one normal subject and three patients with RP are shown in Figure 2. The amplitudes of the fmERGs in case 1 were relatively well preserved, and the macular volume was within the normal range. The amplitudes of the fmERGs in case 2 were reduced, and the macular volume was close to the lower borderline of normal. The fmERGs in case 3 were nonrecordable, and the macular volume was severely reduced.

Box plots of the fmERG amplitudes (a- and b-waves) and total macular volume for 43 normal control subjects and 43 patients with RP are shown in Figure 3. As expected, both the amplitudes of the a- and b-waves of the fmERGs and the total

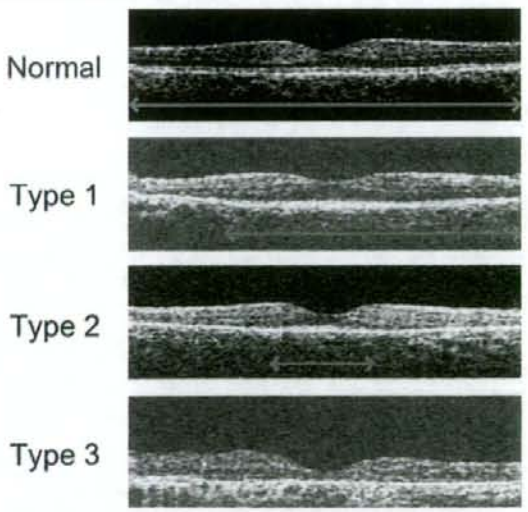

FIGURE 1. The photoreceptor IS/OS junction line in the OCT image can be divided into three categories; type 1, distinct IS/OS line over central 2 mm; type 2, distinct IS/OS line only within central 2 mm; type 3, absent IS/OS line. *Red lines*: the length of the IS/OS line, which was detected on the gray-scale OCT image.

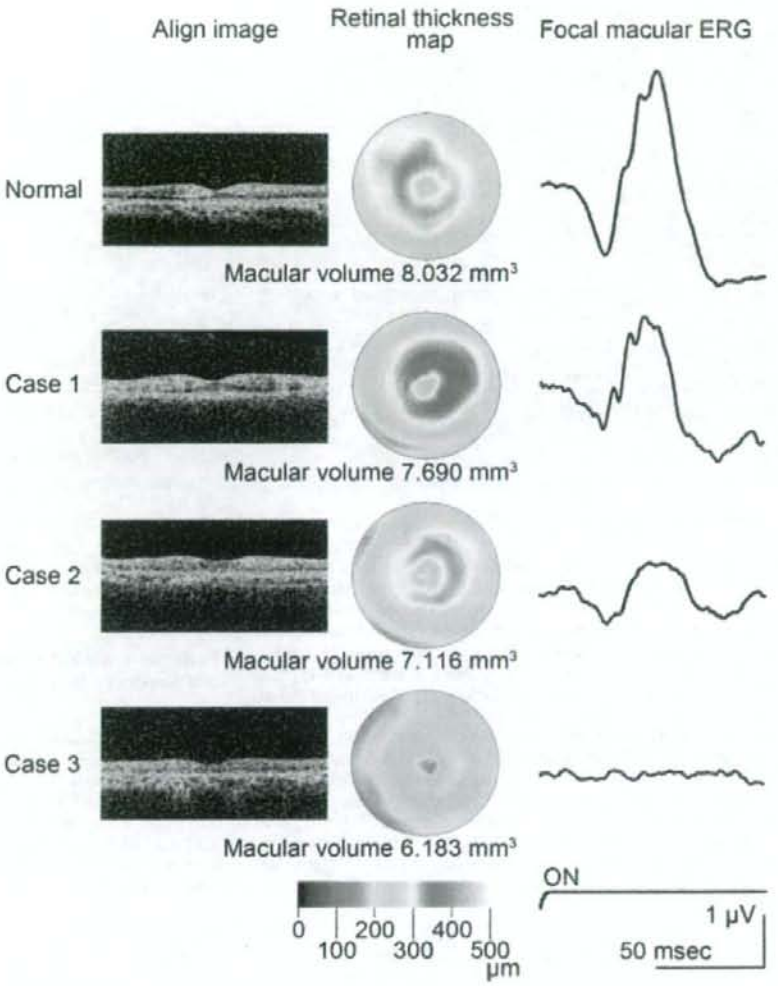

FIGURE 2. OCT images and fmERGs recorded from a normal subject and three representative patients with RP.

macular volume in patients with RP were significantly smaller than those of normal subjects ($P < 0.001$).

Correlation between Amplitude of fmERG and Macular Volume

Because changes in the macular morphology should lead to functional changes,[52] we investigated whether there was a correlation between the amplitude of fmERGs and the total macular volume in our 43 patients with RP. The amplitudes of the a- and b-waves for 43 patients with RP are plotted against the total macular volume in Figures 4A and 4B, respectively. For both graphs, the gray area shows the 2.5 to 97.5 percentiles of normal control subjects.

A significant but weak correlation was found between the fmERG amplitude and total macular volume (a-wave, $\rho = 0.458$, $P < 0.01$; b-wave, $\rho = 0.540$, $P < 0.01$; Spearman's rank correlation). One of the reasons for this relatively weak correlation between the fmERG amplitude and total macular volume was that there were four patients with RP who had normal macular volume but severely reduced fmERG (e.g., patients 4–7, Fig. 4). In contrast, there were no patients with RP who had normal a- and b-wave amplitudes with severely reduced macular volume. There were two patients with RP who had normal a-wave amplitude with reduced macular volume, but their macular volumes were still near the lower borderline of normal, and their b-wave amplitudes were lower than the normal range.

Correlation between fmERG and Length of IS/OS Line

We attempted to measure the thickness of each retinal layer (i.e., outer, middle, and inner retinal layers) separately, but found that it was very difficult to identify the border between these layers, especially in patients with relatively advanced stages of RP. The total macular volume is the sum of the volume of the neural retina in the central 6 mm of the retina and was used in the analyses. In addition, we used the length of the photoreceptor inner segment/outer segment junction